International Journal of Current Science Research and Review
ISSN: 2581-8341
Volume 09 Issue 04 April 2026
DOI: 10.47191/ijcsrr/V9-i4-47, Impact Factor: 8.048
IJCSRR @ 2026
www.ijcsrr.org

Free Radical Scavenging Potential of Cobalt Nanoparticles Synthesized from *Ipomoea Batatas* Leaves Extract

Catherine Otitolaiye[*1], Bashiru Ibrahim[2], Mustapha Muhammad[3], Umar Abdussalam[4]
[1,2,3,4] Department of Biochemistry, Faculty of Science, Sokoto State University, Sokoto, Nigeria

ABSTRACT: Synthesizing nanoparticles with high antioxidant capacity through green routes is critical for creating biocompatible antioxidants. This present study investigated the free-radical scavenging potential of cobalt nanoparticles (CoNPs) synthesized from *Ipomoea batatas* leaf extract. Air-dried leaf powder was macerated separately with distilled water and ethanol for 48 h, respectively. The filtrates were lyophilized to give aqueous and ethanol extracts. Total phenolic, flavonoid and tannin contents were quantified on both extracts, followed by DPPH scavenging assay. The ethanol extract that exhibited higher activity was utilized in the synthesis of CoNPs. The NPs were characterized via UV, Fourier transform infrared spectroscopy (FTIR), X-ray diffraction (XRD), and scanning electron microscopy (SEM-EDX) analysis. The results showed that the ethanol extract demonstrated higher DPPH scavenging activity (IC_{50} 66.49 µg/ml) than aqueous extract (IC_{50}: 641.35 µg/ml) and CoNPs (IC_{50}: 175.18 µg/ml). The CoNPs also competed favorably with ascorbic acid for ferric reducing potential. UV absorption peak was observed at 220 nm, corresponding to the surface plasmon resonance of CoNPs. The FT-IR showed characteristic peaks at <800 cm^{-1} which is characteristic of cobalt oxide bond. The XRD and SEM-EDX analyses showed that the CoNPs were nanocrystalline, spherical, and well-dispersed with an average size of 17–22 nm. The study concludes that the synthesized CoNPs exhibited significant *in vitro* antioxidant potential which could be further explored for *in vivo* antioxidant potential.

KEYWORDS: *Ipomoea batatas*, cobalt nanoparticle, characterization, free radical, DPPH

1.0 INTRODUCTION

Endogenous antioxidant compounds have been thoroughly documented for their ability to neutralize free radicals, reduce lipid peroxidation and suppress the risk of oxidative stress [1,2]. Although free radicals, such as hydroxyl (·OH), superoxide anion ($O_2^{\bullet-}$), and peroxyl ($ROO^{\cdot}$) radicals, are part of normal body metabolism, their overproduction usually leads to oxidative stress and oxidative damage [3-6]. Oxidative stress has also been linked to the pathogenesis of chronic conditions, including rheumatoid arthritis, diabetes, atherosclerosis, chronic kidney disease, cardiovascular disease, and neurological degenerative [2,7,8]. As such, there is a growing need to explore different medicinal plants and nanoparticles with high antioxidant capacity to scavenge the free radicals and attenuate oxidative damage.

In recent years, scientists have focused their research on the preparation of metal nanoparticles (NPs) from medicinal plants due to their high sensitivity, small size (<100 nm), low cost and effectiveness in scavenging harmful free radicals [9 - 11]. Earlier findings showed that NPs were initially produced using cost-intensive techniques and several hazardous chemicals which pose adverse effects on the environment. These limitations have been overcome by the use of green synthesis approach which is eco-friendly, non-toxic and the synthesis can easily be upscaled [12-14]. NPs have reportedly been utilized in healthcare industries for drug delivery, new drug formulations, disease diagnosis and treatment [15,16].

Cobalt nanoparticles (CoNPs) are NPs synthesized from medicinal plants. Cobalt is an essential trace element and an integral part of vitamin B12. It is required for the formation of red blood cells and as such, is useful in the treatment of anemia [17]. Studies have shown that CoNPs are nontoxic at low concentrations in the biological systems and have strong inhibitory activities against bacteria, fungi and viruses [17-20]. In addition, CoNPs have been documented to exhibit anti-cancer, anti-oxidant, anti-diabetic, and cytotoxic properties, making them suitable for biomedical research [10,17,21,22].

Ipomoea batatas (Family: Convolvulaceae) is a major staple food widely available in different parts of Africa including Nigeria although the plant originates from America [23,24]. It is very easy to cultivate using the stem and is harvested several times during the year [25]. Studies showed that *I. batatas* is a rich source of essential elements (copper, iron, potassium and manganese), vitamins, carbohydrates and dietary fibers [26]. In Southern Nigeria, the leaves are consumed as vegetables in soups. The leaves are also

International Journal of Current Science Research and Review
ISSN: 2581-8341
Volume 09 Issue 04 April 2026
DOI: 10.47191/ijcsrr/V9-i4-47, Impact Factor: 8.048
IJCSRR @ 2026
www.ijcsrr.org

believed to boost human health and prevent diseases [25,27]. Previous studies also showed *I. batatas* extracts contain flavonoids, alkaloids, terpenoids, saponins and tannins which have been documented to elicit anti-oxidant, anti-microbial, anti-hypertensive, anti-inflammatory, anti-diabetic and anti-anemic properrties [25,27-29]. In addition, the phytochemicals have been reported to act as oxygen quenchers, hydrogen donors, reducing and stabilizing agents**.** The reduction of metal ions by these substances within the plant extracts leads to the formation of several nanomaterials [17**,** 30]. However, there is paucity of scientific information on the *in vitro* antioxidant property of *I. batatas* leaf NPs. Therefore, the current study aims to synthesize CoNPs using *I. batatas* leaf extracts and investigate its ability to scavenge free radicals.

2.0 MATERIALS AND METHODS

2.1 Collection and Preparation of Plant materials

The leaves of *I. batatas* were collected from a homestead garden in Sokoto, washed with distilled water, air-dried and ground with an electric blender. The pulverized leaf powder (100 g) was macerated separately in 1 L of distilled water and absolute ethanol for 48 h at room temperature (25 ± 2 ºC). These were filtered, lyophilized, and stored at 4ºC until further use.

2.2. Quantitative phytochemical Analysis

2.2.1 Estimation of Phenolic Content

The total phenolic content was determined as described [31]. A 200 µL of the aqueous and ethanol extracts were separately mixed with 1.5 mL of 10% Folin-Ciocalteu reagent (FCR). After 5 min of incubation in the dark, 1.5 mL of 5% Na_2CO_3 was added and vortexed. The mixture was allowed to stand for 2 h in the dark. The optical density was measured at 750 nm on a UV-Vis spectrophotometer. Results were expressed as milligrams of gallic acid equivalent (mgGAE) per g of the extract. The calibration curve was prepared at various concentrations 5, 10, 25, 50, 75, 100, 125, and 150 µg/mL made from 1 mg/mL of gallic acid. The assay was performed in triplicates.

2.2.2 Estimation of Flavonoid Content

The flavonoid content was determined using the aluminum chloride colorimetric method [31]. Briefly, 1 mL of the extract was added to 0.3 mL of 5% sodium nitrite. This was allowed to stand for 5 min in the dark. After which 0.3 mL of 10% aluminum chloride was added. This was mixed and the solution was incubated for another 5 min. Then, 2 mL of NaOH (1 M) was carefully introduced and the solution allowed to stay in the dark for 10 min, at ambient temperature. The absorbance was read at 510 nm. The calibration curve was prepared at various concentrations 5, 10, 25, 50, 75, 100, 125, and 150 µg/mL made from 1 mg/mL of quercetin. The total flavonoid content was expressed as milligrams of quercetin equivalent per g of extract (mgQE/g).

2.2.3. Estimation of Tannin Content

The tannin content was quantified using the spectrophotometric method [31]. A volume of 100 µL of the extract was mixed with distilled water (7.5 mL), 0.5 mL of 10% (v/v) FCR, and 1 mL of 35% Na_2CO_3 solution. The mixture was allowed to stand for 10 min at room temperature. Then, the absorbance was read at 725 nm on a UV-Vis spectrophotometer. The calibration curve was prepared at various concentrations 5, 10, 25, 50, 75, 100, 125, and 150 µg/mL made from 1 mg/mL of gallic acid. Results were expressed as milligrams of gallic acid per g of extract.

2.3 Antioxidant Assays

2.3.1 DPPH Scavenging Activity

This assay was performed as reported [31]. Briefly, 0.3 mM DPPH radical solution was prepared in methanol. Then, 1 mL of the extract or CoNPs was added to 2 mL of DPPH solution in triplicates. The reaction mixture was vortexed and incubated in the dark for 30 min and the absorbance was read at 517 nm. The same procedure was repeated for gallic acid standard at concentrations of 5, 10, 20, 40, 80, 160, and 320 µg/mL. Thereafter, the percentage inhibition of DPPH radical was calculated as follows:

$$\%\ Inhibition\ of\ DPPH\ radical = \frac{\text{Abs of control} - Abs\ of\ extract/standard}{\text{Abs of control}}\ X\ 100$$

2.3.2 Ferric Reducing Antioxidant Power (FRAP) Test

The ferric reducing antioxidant power of the test samples was determined based on standard method [32]. To 0.5 ml of the ascorbic acid or CoNPs (0.2 – 1.0 mg/mL) was added 1.25 mL of 0.2 M phosphate buffer (pH 6.6) and 1.25 mL of 1% potassium ferricyanide. These were thoroughly mixed and incubated at 50ºC for 30 min. Thereafter, 1.25 mL of 10% trichloroacetic acid was added and the

International Journal of Current Science Research and Review
ISSN: 2581-8341
Volume 09 Issue 04 April 2026
DOI: 10.47191/ijcsrr/V9-i4-47, Impact Factor: 8.048
IJCSRR @ 2026
www.ijcsrr.org

mixture was centrifuged at 3000 rpm for 10 min. The supernatant was separated and 0.625 mL of the supernatant was mixed with 0.625 mL of distilled water and 0.125 mL of 0.1% $FeCl_3$. The absorbance was measured at 700 nm against blank. The experiment was performed in triplicate.

2.4 Green synthesis of cobalt nanoparticles (CoNPs) from *I. batatas*

The cobalt NPs were synthesized from the ethanol leaf extract of *I. batatas* as described by Malathy and Revathi [22]. Briefly, 100 mL of 1% cobalt nitrate solution was mixed with 10 mL of *I. batatas* ethanol leaf extract on a magnetic stirrer at 50 ºC for 30 min. The color of the solution changed from pink to dark brown indicating the formation of CoNPs. Thereafter, the CoNP was centrifuged and the pellet was oven dried at 50ºC. The dried sample was kept in a desiccator until when used.

2.5 Characterization of CoNPs

2.5.1 UV Spectroscopic Method

The CoNP was characterized on a UV-Visible spectrophotometer (Model ASUV-6300PC) at various wavelengths 200 -1000 nm. An aliquot of the sample was dissolved in methanol and filtered. The absorbance of the filtrate was scanned at various wavelengths (200 -1000 nm) using the quartz cuvette for maximum absorption.

2.5.2 X-Ray Diffraction (XRD) Analysis

The XRD analysis was performed to determine the crystalline structure of the CoNPs. The analysis was performed on Rigaku MiniFlex 6G, 300/600 diffractometer equipped with Rigaku SmartLab software, operated at 40 kV and 15 mA with Cu Kα radiation ($\lambda = 0.15406$ nm). The diffraction data were collected over a 2θ range of 3-90° with a step size of 0.01°.

2.5.3 Fourier transform infrared spectroscopy (FT-IR)

The FT-IR analysis was conducted to identify the various functional groups in the CoNPs using an Agilent Cary 630 FT-IR spectrometer. The system utilized a high-emission infrared radiation source in transmittance mode, with signals collected within the range of 4000-650 cm^{-1}. The sample spectra were acquired and processed using MicroLab software.

2.5.4 SEM-EDX Analysis

For morphological and elemental characterization, the sample was mounted on stubs with adhesive carbon tape and coated with 20 nm of carbon using a Quorum Q150R ES mini sputter coater. The prepared sample was then analyzed with a Phenom PRO-X SEM, equipped with an Oxford XMax 50 Silicon Drift Energy Dispersive X-ray (EDX) detector. The analysis was performed at an accelerating voltage of 15 kV under high vacuum conditions.

2.6 Statistical Analysis

Results were expressed as the mean ± standard error of the mean (SEM). Statistical analysis was performed using GraphPad Prism (version 10.0). Comparisons between groups were analyzed using Student's t-test or one-way analysis of variance (ANOVA), followed by appropriate post-hoc tests where applicable. A p-value of $p < 0.05$ was considered statistically significant.

3.0 RESULTS

3.1 Phytochemical analysis

The quantitative analysis of the phytocompounds in *I. batatas* revealed the ethanol extract contained significant ($p<0.05$) amounts of of phenols and flavonoids compared to the aqueous extract (Table 1).

Table 1: Results of quantitative phytocompounds of *I. batatas* aqueous and ethanol leaves extracts

	Aqueous extract	Ethanol extract
Phenolics (mgGAE/g of extract)	20.98 ± 3.34	187.68 ± 10.97***
Flavonoids (mgQE/g of extract)	52.45 ± 3.19	209.45 ± 15.39***
Tannin (mgGAE/g of extract)	41.58 ± 3.29	77.14 ± 7.38*

Values are mean ± SEM (n = 3). The superscript (*) indicate values that are significantly ($p < 0.05$) different for each phytochemical.

International Journal of Current Science Research and Review
ISSN: 2581-8341
Volume 09 Issue 04 April 2026
DOI: 10.47191/ijcsrr/V9-i4-47, Impact Factor: 8.048
IJCSRR @ 2026
www.ijcsrr.org

3.2 DPPH Scavenging Activity

The ethanol extract of *I. batatas* significantly ($p<0.05$) scavenged the DPPH radicals (IC_{50}: 66.49 µg/ml) than the CoNPs (IC_{50}: 175.18 µg/ml) and the aqueous extract (IC_{50}: 641.35 µg/ml). However, both the extracts and the CoNPs were found to be significantly weaker than the gallic acid standard (IC_{50}: 0.018 µg/ml) as shown in Figure 1.

3.3 FRAP

The CoNPs also elicited ferric reducing antioxidant potential and competed effectively with ascorbic acid standard. As shown in Figure 2, as the concentration increased, the absorbance also increased.

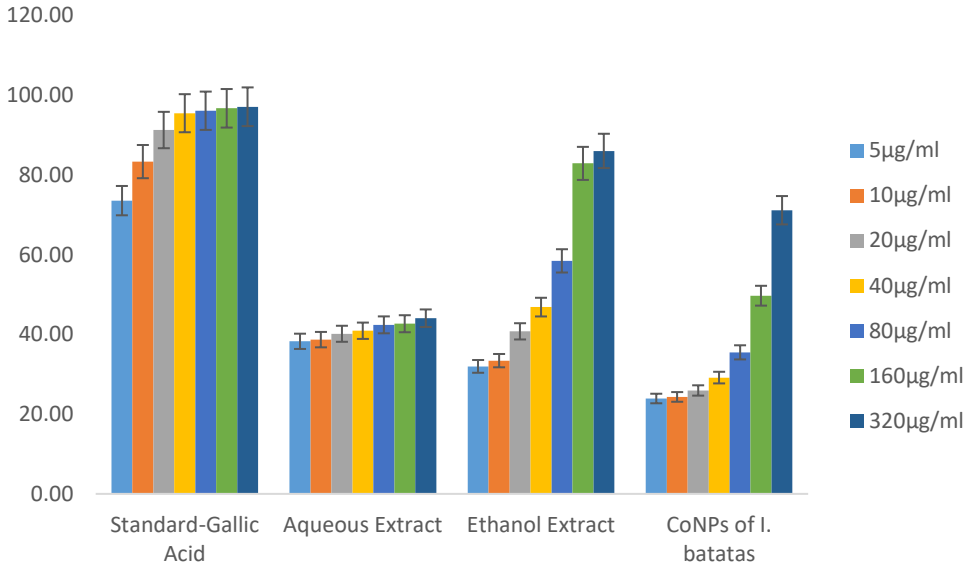

Fig 1: DPPH radical scavenging ability of *I. batatas* extracts and its cobalt nanoparticle. Data are mean ± SEM of triplicate determinations. The error bars are 5% of the mean values.

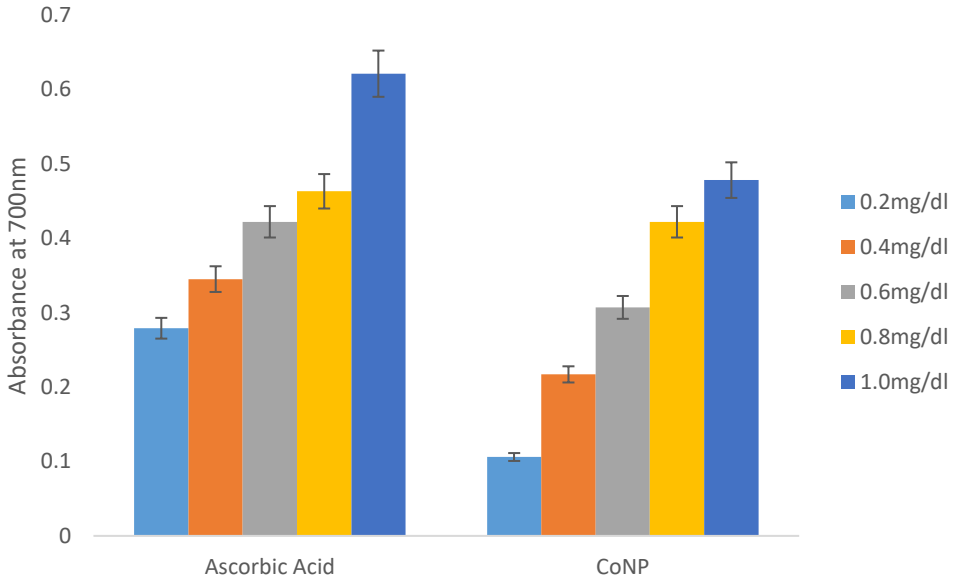

Figure 2: Ferric reducing antioxidant potential of cobalt nanoparticle synthesized from *I. batatas* and the reference standard (ascorbic acid). Data are mean ± SEM of triplicate determinations. The error bars are 5% of the mean values.

International Journal of Current Science Research and Review
ISSN: 2581-8341
Volume 09 Issue 04 April 2026
DOI: 10.47191/ijcsrr/V9-i4-47, Impact Factor: 8.048
IJCSRR @ 2026
www.ijcsrr.org

3.3 UV Absorption Spectrum of CoNPs

The Figure 3 showed the UV absorption spectrum of the CoNPs at 200 – 1000 nm. The absorption spectrum (Figure 3) exhibited a distinct maximum absorption peak at approximately 220 nm, characteristic of the surface plasmon resonance of cobalt nanoparticles synthesized via green routes. Following the primary peak at 220 nm, there was a steady decline in absorbance as the wavelength increased toward the visible and near-infrared (NIR) regions (400 - 1000 nm). The absence of broad, messy peaks in the visible range suggests that the sample is relatively homogeneous and free from large, irregular aggregates that would typically cause scattering at higher wavelengths. Therefore, the smooth decline in absorbance throughout the visible spectrum suggested stability of the nanoparticles. Furthermore, the sharp peak in the shorter wavelength region of the spectrum indicated the presence of capping agents (like phenolics) and the successful formation of very small, fine nanoparticles.

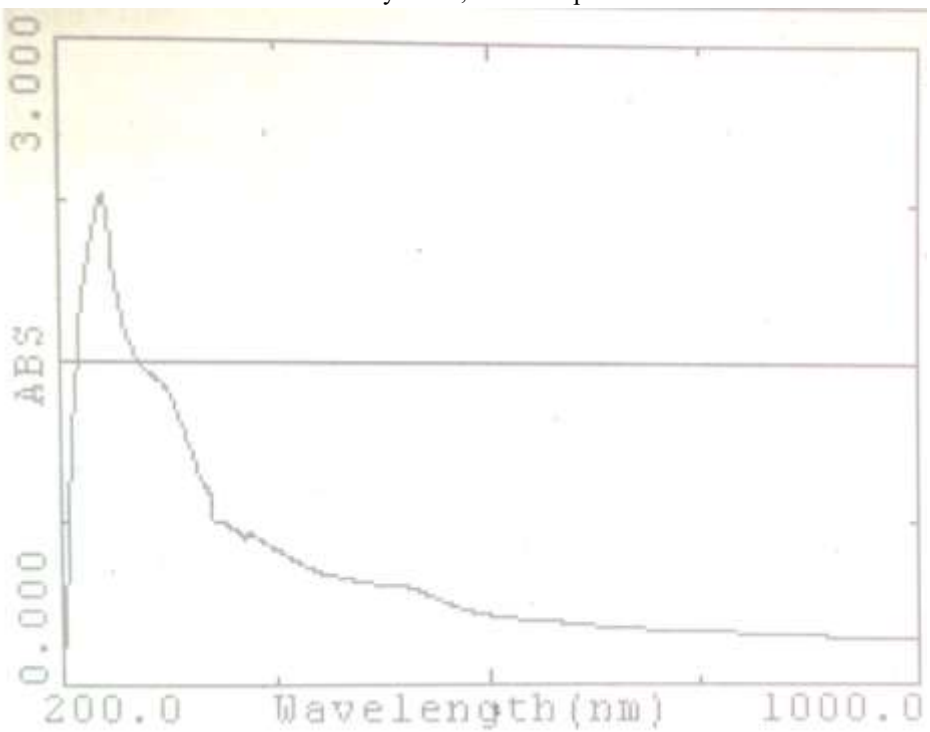

Figure 3: UV-Visible absorption spectrum of synthesized cobalt nanoparticles (CoNPs).

The UV-Vis spectrum shows the characteristic optical properties of the CoNPs synthesized via the green route. A prominent absorption peak was observed at 220 nm, corresponding to the surface plasmon resonance (SPR) of the cobalt nanoparticles. The sharp nature of the peak suggests a narrow size distribution, while the absence of significant secondary peaks at higher wavelengths indicates the stability of the colloidal suspension and the successful role of plant-derived biomolecules as capping and stabilizing agents.

3.4 X-Ray Diffraction

The crystalline structure and phase purity of the green-synthesized CoNPs were analyzed using XRD, as shown in Figure 4. The diffractogram exhibited a series of well-defined Bragg reflections at 2 θ values of 17.57°, 20.79°, 25.89°, 30.09°, 34.32°, 44.36°, 52.12°, and 54.56°. The corresponding interplanar spacings (d-values), calculated using Bragg's law, range from 5.05 Å to 1.68 Å. All diffraction peaks exhibited significant broadening, with Full Width at Half Maximum (FWHM) values ranging between 0.38° to 0.46°. This peak broadening is characteristic of small crystallite sizes and limited long-range structural order within the nanoparticles. The average crystallite size, estimated using the Scherrer equation from the primary diffraction peaks, was approximately 22 nm (range: 18–23 nm), confirming the nanocrystalline nature of the synthesized material.

International Journal of Current Science Research and Review
ISSN: 2581-8341
Volume 09 Issue 04 April 2026
DOI: 10.47191/ijcsrr/V9-i4-47, Impact Factor: 8.048
IJCSRR @ 2026
www.ijcsrr.org

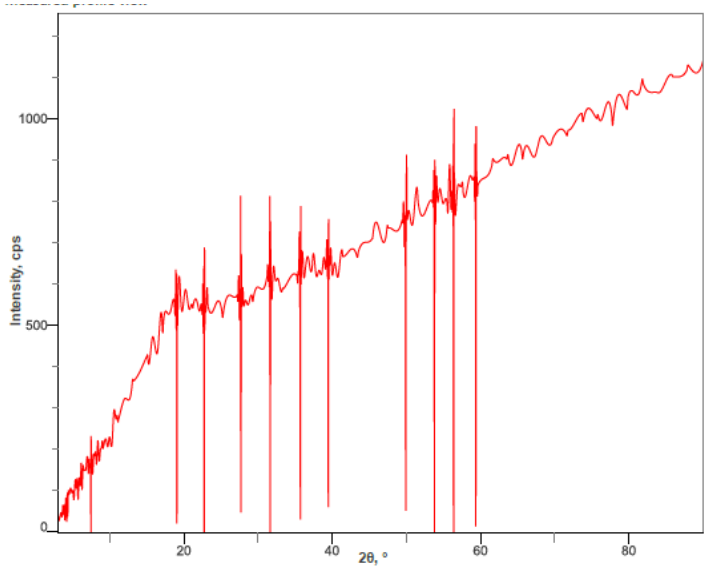

Fig 4: XRD pattern of synthesized CoNPs from *I. batatas* ethanol leaf extract.

3.5 FT-IR Absorption Spectrum

The FTIR analysis was employed to identify the biomolecules involved in the capping and stabilization of the synthesized cobalt nanoparticles as shown in Figure 5. The FTIR spectrum exhibited several characteristic absorption bands corresponding to oxygenated and hydrocarbon-based functional groups. A broad, intense absorption band observed between 3362 and 3229 cm^{-1} was attributed to O-H stretching vibrations, indicating the presence of hydroxyl-containing compounds such as alcohols or phenolics. The absorption band at 1619 cm^{-1} is assigned to C=C aromatic skeletal vibrations or C=O (Amide I) stretching, suggesting the presence of aromatic compounds or proteins. The absence of a strong absorption band in the 1700–1750 cm^{-1} region suggested that free carbonyl-containing functional groups, such as esters or ketones were minimal. A prominent band at 1036 cm^{-1} corresponds to C-O stretching vibrations, which further supported the presence of alcohols or phenolic compounds and the oxygenated nature of the sample. In the fingerprint region, absorption bands at 910 cm^{-1} and 743 cm^{-1} were linked to out-of-plane C-H bending vibrations, typical of substituted aromatic rings. Additionally, the peaks in the lower frequency region (<800 cm^{-1}) could likely be associated with Co-O metal-oxygen bonds, confirming the successful formation of cobalt-based nanostructures.

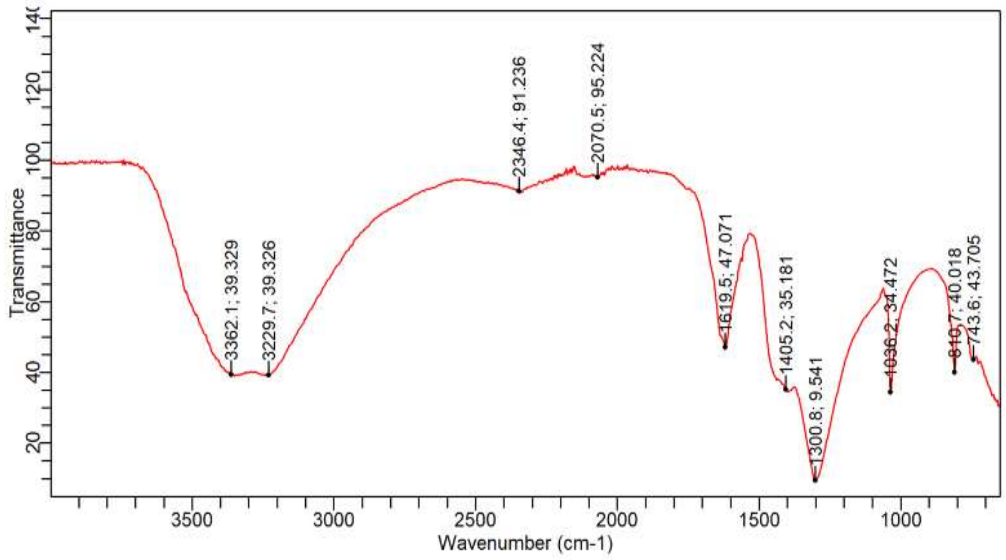

Fig 5: FT-IR spectrum of CoNPs synthesized from *I. batatas* extract

International Journal of Current Science Research and Review
ISSN: 2581-8341
Volume 09 Issue 04 April 2026
DOI: 10.47191/ijcsrr/V9-i4-47, Impact Factor: 8.048
IJCSRR @ 2026
www.ijcsrr.org

3.6 Surface Morphological Analysis of CoNPs (SEM-EDX)

The surface topography and morphological features of the synthesized cobalt nanoparticles (20 nm scale) were investigated using scanning electron microscopy (SEM) (Figure 6a). The micrograph showed that the nanoparticles possessed a spherical morphology with a uniform and smooth surface. The particles appear well-dispersed, which suggests that the bio-organic capping agents effectively reduced surface energy and prevented significant agglomeration. Measurement of individual particles yielded sizes of ~17.3 nm, which was consistent with (22 nm nanocrystalline domains estimated from the XRD data.

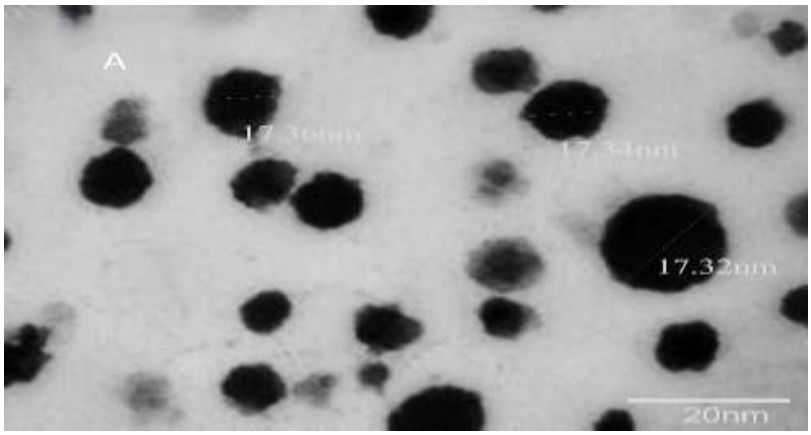

Fig 6a: TEM at 20nm of cobalt nanoparticle synthesized from *I. batatas*

At 50 nm scale bar (Figure 6b), the cobalt nanoparticles were relatively well dispersed. Particle size measurements showed an average diameter of ~15-17 nm. At the 100 nm scale bar (Figure 6c), the cobalt nanoparticles appeared larger and more clearly defined compared to the lower magnification images. Instead of showing several tiny individual particles, some of the nanoparticles seemed to form small clusters. The observed size ranged between ~38 and 50 nm.

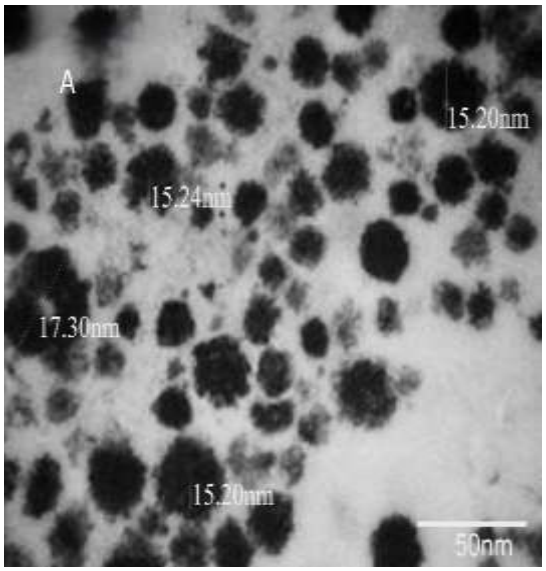

Fig 6b: TEM at 50nm of cobalt nanoparticle from *I. batatas*

The SEM micrographs (Figure 7b) revealed the presence of a heterogeneous particulate surface composed of clustered, sphere-like features distributed across the substrate. At lower magnification (360x, 200 µm scale bar), the surface appeared discontinuous particle-rich domains with bright contrast regions corresponding to cobalt-containing material. These regions suggested that the

International Journal of Current Science Research and Review
ISSN: 2581-8341
Volume 09 Issue 04 April 2026
DOI: 10.47191/ijcsrr/V9-i4-47, Impact Factor: 8.048
IJCSRR @ 2026
www.ijcsrr.org

nanoparticles were not completely isolated but instead formed interconnected assemblies. This morphology could be an indication of the presence of nanoparticles forming compact clusters.

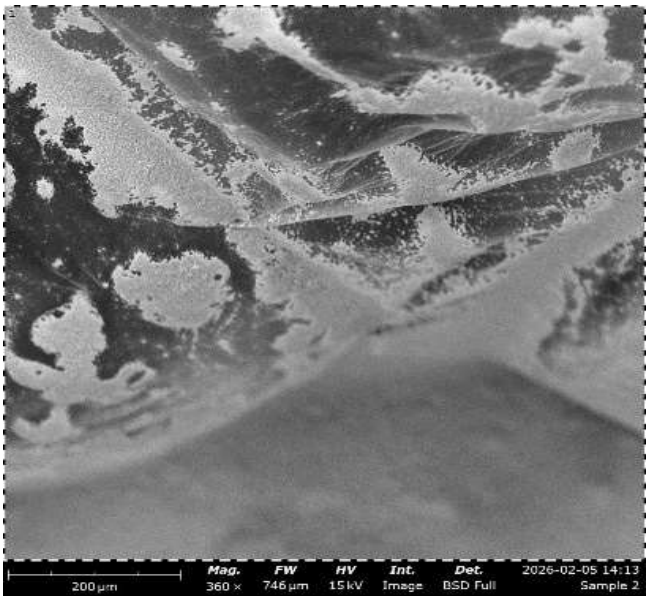

Fig 7a: SEM at 360x of cobalt nanoparticle from *I. batatas*

At higher magnification (1500×; 50 µm scale bar), the clustered morphology became more visible (Figure 7c). Dense agglomerates with rough surface textures were visible. Individual primary nanoparticles were not fully resolved at this magnification. However, the nodular surface structure confirmed that smaller particles were assembled into larger micro-scale aggregates.

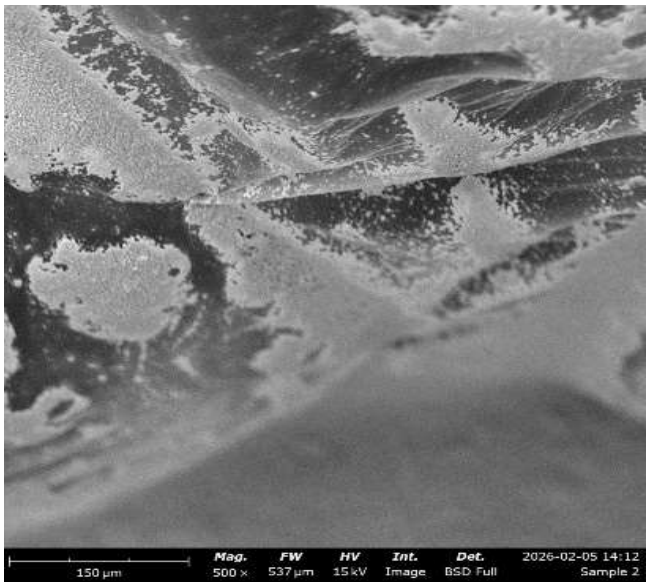

Fig 7b: SEM at 500x of cobalt nanoparticle from *I. batatas*

International Journal of Current Science Research and Review
ISSN: 2581-8341
Volume 09 Issue 04 April 2026
DOI: 10.47191/ijcsrr/V9-i4-47, Impact Factor: 8.048
IJCSRR @ 2026
www.ijcsrr.org

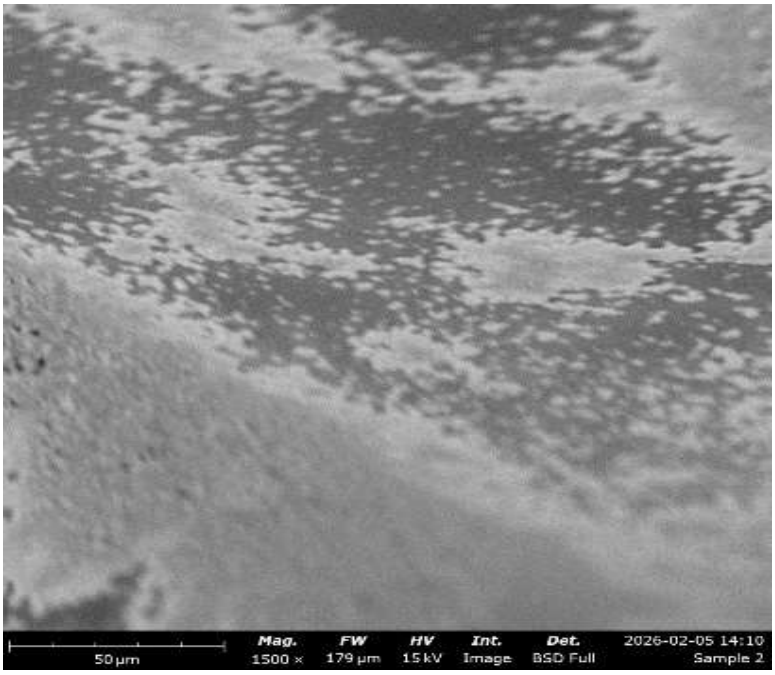

Fig 7c: SEM at 1500X of cobalt nanoparticle from *I. batatas*

4.0 DISCUSSION

The extracts' capacity to scavenge free radicals could be attributed to the presence of phytoconstituents. This study demonstrated that the ethanol extract contained significant phytochemicals, including phenols, flavonoids and tannins. Studies have shown that flavonoids, phenols, and tannins are polyphenolic compounds with potent antioxidant properties as metal chelating and reducing agents, singlet oxygen quenchers, and donors of hydrogen or electrons [13,33,34].

This study has shown that the synthesized CoNPs were effective at scavenging DPPH radicals and reducing of ferric (Fe^{3+}) to ferrous (Fe^{2+}) ions. Previous studies reported that increase in absorbance at 700 nm equals to increase in the reducing power of the extract or herbal preparation [35-37]. The observation in this study suggested that the CoNPs from *I. batatas* could serve as a potential antioxidant to protect against oxidative stress-related conditions [38-39].

The optical properties of the synthesized CoNPs, as characterized by UV-Vis spectroscopy, provided a significant insight into the formation and stability of the nanoparticles. The emergence of a distinct peak at 220 nm was a hallmark of metallic cobalt nanostructures in a colloidal state. This sharp resonance in the UV region was consistent with the presence of very small, fine nanoparticles, which is further corroborated by the average crystallite size of 22 nm derived from the XRD data.

The steady, monotonic decline in absorbance from 400 to 1000 nm, combined with the absence of broad absorption bands in the visible spectrum, indicated a high degree of sample homogeneity. In nanoparticle synthesis, the lack of secondary peaks at higher wavelengths is a critical indicator that the system is free from large, irregular aggregates or polydispersed clusters that typically induce Mie scattering.

Furthermore, the stability of the colloidal suspension could be attributed to efficient capping effect of phytoconstituents, such as phenolics and flavonoids. As indicated by the FTIR results, these oxygenated biomolecules form a protective layer around the cobalt nuclei, reducing the surface energy and preventing agglomeration. This synergistic relationship between the small particle size observed at 220 nm and the stabilizing matrix of the extract underscored the efficiency of the green synthesis approach. Previous findings maximum absorption peak for CoNPs at 300 nm [40,41], possibly due to the nature of the constituents and functional groups present.

The XRD diffractogram confirmed the crystalline nature of the green-synthesized CoNPs, showing well-defined Bragg reflections. The calculated d-spacings (5.05–1.68 Å) and significant peak broadening were characteristic of nanocrystalline structures with limited long-range order. Using the Scherrer equation, the average crystallite size was estimated at **22 nm**. This small particle size

International Journal of Current Science Research and Review
ISSN: 2581-8341
Volume 09 Issue 04 April 2026
DOI: 10.47191/ijcsrr/V9-i4-47, Impact Factor: 8.048
IJCSRR @ 2026
www.ijcsrr.org

is significant for biological applications, as the resulting high surface-area-to-volume ratio typically enhances the bioavailability and therapeutic efficacy of the nanoparticles, correlating well with the results obtained from UV-Vis and SEM analyses [13, 40-42]. Peaks observed between 20° and 35° 2θ reflect short-range molecular ordering, while the gradual reduction in peak intensity at higher angles was an indication for an increasing disorder at smaller lattice spacings. The broad amorphous background observed across the diffractogram confirmed that a significant fraction of the material lacked long-range order. This behavior is typical of organic materials and reaction products, where partial crystallization occurs within an amorphous matrix.

FTIR analysis identified the specific functional groups responsible for the reduction and stabilization of the CoNPs. The broad band at 3362–3229 cm^{-1} (O-H stretching) and the peak at 1619 cm^{-1} (C=C aromatic or C=O amide stretching) confirmed that polyphenols and proteins from the *I. batata* extract were the primary capping agents [40,42]. The absence of peaks in the 1700–1750 cm^{-1} range indicated a lack of free carbonyls, suggesting these groups were actively involved in the stabilization process [43,44]. Furthermore, the prominent 1036 cm^{-1} (C-O stretching) and fingerprint peaks at 910–743 cm^{-1} verify the presence of a robust organic matrix. Crucially, the peaks below 800 cm^{-1} were attributed to Co-O metal-oxygen bonds, confirming the successful transition from plant-derived precursors to cobalt-based nanostructures. This organic coating not only prevents agglomeration but also likely enhanced the biocompatibility of the particles for pharmacological use.

The surface morphology and topography of the CoNPs were further elucidated via SEM analysis which revealed predominantly spherical particles with smooth, uniform surfaces. The high degree of dispersion observed in the micrographs suggested that the bio-organic capping agents identified in the FTIR analysis effectively reduced the surface energy, thereby preventing significant agglomeration. Individual particle measurements yielded a size of approximately 17.3 nm, which is in close agreement with the 22 nm nanocrystalline domains estimated from the XRD data. This consistency across multiple characterization techniques robustly confirmed the successful synthesis of stable, monodispersed cobalt nanostructures with a high surface-area-to-volume ratio [13,40,44,45,46].

5.0 CONCLUSION

This study successfully demonstrated the green synthesis of cobalt nanoparticles (CoNPs) using *Ipomoea batatas* leaf extract as a sustainable reducing and stabilizing agent. Comprehensive characterization revealed that the CoNPs were nanocrystalline, predominantly spherical, and well-dispersed with an average size of 17–22 nm. The presence of a bio-organic capping matrix, confirmed by FTIR, effectively stabilized the nanoparticles and prevented significant agglomeration. Furthermore, the synthesized CoNPs exhibited considerable antioxidant potential *in vitro*, suggesting their promise as therapeutic agents. These findings provide a strong foundation for future *in vivo* studies to evaluate their efficacy against oxidative stress-related and inflammatory diseases.

Conflict of Interest

The authors declare no conflict of interest.

Acknowledgment

This study was supported by the Tertiary Education Trust Fund (TETFUND) on the award of IBR grant for Year 2025 to Sokoto State University Sokoto.

The authors wish to thank Dr. Godwin Anyim of the Federal University of Health Sciences, Ila Orangun Osun State, Nigeria for proofreading this manuscript and offering his valuable comments.

Limitation of the study

The EDX results were not presented due to technical glitches encountered during the analysis. This would be resolved in subsequent studies.

REFERENCES

1. Shahidi, F. (2012) Nutraceuticals, functional foods and dietary supplements in health and disease. *J. Food Drug Anal.* 20(1): 226-230 https://doi.org/10.38212/2224-6614.2144
2. Farooq, M.U., Mumtaz, M.W., Mukhtar, H., Rashid, U, Akhtar, M.T., Raza, S.A. and Muhammad Nadeem, M. (2020) UHPLC-QTOF-MS/MS based phytochemical characterization and anti-hyperglycemic prospective of hydro-ethanol leaf extract of *Butea monosperma. Scientific Reports: Nature Research.*10:3530 https://doi.org/10.1038/s41598-020-60076-5

International Journal of Current Science Research and Review
ISSN: 2581-8341
Volume 09 Issue 04 April 2026
DOI: 10.47191/ijcsrr/V9-i4-47, Impact Factor: 8.048
IJCSRR @ 2026
www.ijcsrr.org

3. Halliwell, B. (2011) Free radicals and antioxidants – quo vadis? *Trends Pharmacol. Sci*. 32(3):125 – 130 DOI: 10.1016/j.tips.2010.12.002
4. Sudha, G., Sangeetha Priya, M., Indhu, S R. and Vadivukkarasi, S. (2011) In vitro free radical scavenging activity of raw pepino fruit (*Solanum muricatum aiton*). *Int J Curr Pharm Res:* 137-140.
5. Rahman, T., Hosen, I., Towhidul-Islam, M. M. and Shekbar, H.U. (2012) Oxidative stress and human health. *Advances in Bioscience and Biotechnology*. 3(7): 997-1019 DOI: 10.4236/abb.2012.327123
6. Ye, Z.W., Zhang, J., Townsend, D.M. and Tew, K.D. (2015) Oxidative stress, redox regulation and diseases of cellular differentiation. *Biochim. Biophys. Acta* 1850(8): 1607 – 1621 DOI: 10.1016/j.bbagen.2014.11.010
7. Agarwal, A., Aponte-Mellado, A., Premkumar, B.J., Shaman, A. and Gupta, S. (2012). The effects of oxidative stress on female reproduction: a review. *Reproductive Biology and Endocrinology*. 10:49. doi: 10.1186/1477-7827-10-49
8. Otitolaiye, C.A., Makusidi, A.M., Ndodo, N.D., Labbo, A.M. and Bashiru, I. (2019) Role of oxidative stress in glycated hemoglobin among chronic kidney disease (CKD) patients in Sokoto. *IOSR Journal of Dental and Medical Sciences (IOSR-JDMS)*. 18(5): 69-75 DOI:10.9790/0853-1805066975
9. Cardoso, V.F., Francesko, A., Ribeiro, I., Bañobre-López, M., Martins, P. and Lanceros-Mendez, S. (2018) Advances in magnetic nanoparticles for biomedical applications. *Adv Healthcare Mater*. 7(5):1700845. doi: 10.1002/adhm.201700845
10. Azharuddin, M., Zhu, G.H., Das, D., Ozgur, E., Uzun, L. and Turner, A.P. (2019) A repertoire of biomedical applications of noble metal nanoparticles. *Chem Commun.*55(49): 6964–96. Doi: 10.1039/C9CC01741K
11. Das, D. and Saikia, B.J. (2023) Synthesis, characterization and biological applications of cobalt oxide (Co_3O_4) nanoparticles. *Chemical Physics Impact* 6:100137. doi.org/10.1016/j.chphi.2022.100137
12. Dhuper, S., Panda, D. and Nayak, P.L. (2012) Green synthesis and characterization of zero valent iron nanoparticles from the leaf extract of *Mangifera indica*. *Nano Trends: J Nanotech App* 13(2):16–22.
13. Ahmed, K., Tariq, I., Siddiqui, S.U. and Mudassir, M. (2016) Green synthesis of cobalt nanoparticles by using methanol extract of plant leaf as reducing agent. *Pure and applied biology*. 5(3): 453-457 http://dx.doi.org/10.19045/bspab.2016.50058
14. Oyeniyi, Y.J. and Mumuni, A.M. (2021) Formulation development of an herbal hand sanitizer containing Moringa oleifera silver nanoparticles. *Brazilian Journal of Technology, Curitiba*. 4(1):36-49 DOI:10.38152/bjtv4n1-003
15. Parveen, S., Misra, R. and Sahoo, S.K. (2012) Nanoparticles: a boon to drug delivery, therapeutics, diagnostics and imaging. *Nanomedicine: Nano Technol. Biol. Med*. 8(2):147-166 doi:10.1016/j.nano.2011.05.016
16. Smith, D.M., Simon, J.K. and Baker Jr, J.R. (2013) Applications of nanotechnology for immunology. *Nat Rev Immunol*. 13(8):592–605. DOI: 10.1038/nri3488
17. Waris, A., Din, M., Ali, A., Afridi, S., Baset, A., Khan, A.U. and Ali, M. (2021) Green fabrication of Co and Co_3O_4 nanoparticles and their biomedical applications: A review. *Open Life Sciences.* 16: 14–30 https://doi.org/10.1515/biol-2021-0003
18. Ansari, S.M., Bhor, R.D., Pai, K.R., Sen, D., Mazunder, S., Ghosh, K., Kolekar, Y.D. and Ramana, I.V. (2017) Cobalt nanoparticles for biomedical applications: Facile synthesis, physiochemical characterization, cytotoxicity behavior and biocompatibility. S0169433217306530.https://www.sciencedirect.com/science/article/pii/S0169433217306530
19. Adekunle, A.S., Oyekunle, J.A.O., Durosinmi, L.M., Oluwafemi, O.S., Olayanju, D.S., Akinola, A.S., Obisesan, O.R., Akinyele, O.F., and Ajayeoba, T.A. (2020) Potential of cobalt and cobalt oxide nanoparticles as nanocatalyst towards dyes degradation in wastewater. *Nano-Struct, Nano-Objects* 21: 100405.
20. Eleraky, N.E., Allam, A., Hassan, S.B. and Omar, M.M. (2020) Nanomedicine fight against antibacterial resistance: an overview of the recent pharmaceutical innovations. *Pharmaceutics*. 12(2):142. doi: 10.3390/pharmaceutics12020142
21. Padigya, P.R.M., Koyyati, R. and Kudle, K.R. (2016) Evaluation of Antibacterial and cytotoxic activity of green synthesized cobalt nanoparticles using *Raphanus sativus var. longipinnatus* leaf extract. *Int.J. PharmTech Res*. 9(3):466-472.
22. Malathy, D. and Revathi, M. (2021) Green synthesis of cobalt nanoparticles using ethanolic extract of Cadiospermum halicacebium characterization and its anticancer applications. *Research Journal of Pharmacy and Technology*. 14(3):1530-1534. DOI: 10.5958/0974-360X.2021.00271.7

23. Abidin, P.E. (2004) Sweet potato breeding for northeastern Uganda: Farmer varieties, farmer-participatory selection, and stability of performance (PhD Thesis). The Netherlands: *Wageningen University*. Pp 152 *ISBN 90-8504-033-7*.
24. Escobar-Puentes, A.A., Palomo, I., Rodríguez, L., Fuentes, E., Villegas-Ochoa, M.A., González-Aguilar, G.A., Olivas-Aguirre, F.J. and Wall-Medrano, A. (2022) Sweet Potato (*Ipomoea batatas* L.) Phenotypes: From Agroindustry to Health Effects. Foods. 11(7): 1058 doi: 10.3390/foods11071058
25. Alam, M.A. (2021) A comprehensive review of sweet potato (Ipomoea batatas [L.] Lam): Revisiting the associated health benefits. *Trends in Food Science & Technology*. 115: 512-529, ISSN 0924-2244 https://doi.org/10.1016/j.tifs.2021.07.001.
26. Pochapski M.T., Fosquiera E.C,, Esmerino L.A., dos Santos E.B., Farago P.V., Santos F.A., and Groppo F.C. (2011) Phytochemical screening, antioxidant, and antimicrobial activities of the crude leaves' extract from Ipomoea batatas (L.) Lam. *Pharmacogn Mag*. 7(26):165–170 doi: 10.4103/0973-1296.80682
27. Mohanraj, R. and Sivasankar, S. (2014) Sweet Potato (Ipomoea batatas [L.] Lam) - A valuable medicinal food: A review. *J. Med. Food*. 17(7):733–741 doi: 10.1089/jmf.2013.2818
28. Meira, M., Da Silva, E.P., David, J.M., David J.P. (2012) Review of the genus Ipomoea: Traditional uses, chemistry, and biological activities. *Rev. Bras. Farmacogn.* 22: 682–713 https://doi.org/10.1590/S0102-695X2012005000025
29. Wang, S., Nie, S. and Zhu, F. (2016) Chemical constituents and health effects of sweet potato. *Food Res. Int.* 89(1): 90–116 DOI: 10.1016/j.foodres.2016.08.032
30. Dwivedi AD, Gopal K. Biosynthesis of silver and gold nanoparticles using Chenopodium album leaf extract. Colloids Surf A. 2010 Oct 20;369(1–3):27–33.
31. Otitolaiye, I., Omonkhua, A., Oriakhi, K., Okello, E., Onoagbe, I. and Okonofua, F. (2023) Phytochemical analysis and in vitro antioxidant potential of aqueous and ethanol extracts of *Irvingia gabonensis* stem bark. *Pharmacog Res.* 15(2):363-72. DOI:10.5530/pres.15.2.039
32. Akinpelu B.A., Godwin A., Gbadegesin T., Ajakaye N., Omotosho S.E., Azeez S.O., Oziegbe M. and Oyedapo O.O. (2019) Comparative studies on the anti-inflammatory, antioxidant and anti-mutagenic activities of *Crassocephalum crepidioides* (Bent) leaf cold and hot water extracts. *Asian Food Science Journal* 9(1): 1-12 doi:10.9734/AFSJ/2019/v9i130000
33. Diniyah, N. and Lee, S.-H. (2020) Phenolic composition and antioxidant potential of legumes – a review. *J. Agroteknologi*, 14(1): 91–102 doi: 10.19184/j-agt.v14i01.17965.
34. Rice-Evans, C (2004). Flavonoids and Isoflavones: absorption, metabolism and bioactivity. *Free Rad Biol* 36(7): 827-828. DOI: 10.1016/j.freeradbiomed.2003.12.012
35. Ou B., Huang D., Hampsch-Woodill M., Flanagan J.A. and Deemer E.K. (2002) Analysis of antioxidant activities of common vegetables employing Oxygen Radical Absorbance Capacity (ORAC) and Ferric Reducing Antioxidant Power (FRAP) assays: A comparative study. *J Agric Food Chem.* 50(11):3122-8. doi: 10.1021/jf0116606, PMID 12009973.
36. Huang D., Ou B. and Prior R. L (2005). The chemistry behind antioxidant capacity assays. *J Agric Food Chem.* 53(6):1841-56. doi: 10.1021/jf030723c, PMID 15769103.
37. Adebiyi O.E., Olayemi F.O., Ning-Hua T. and Guang-Zhi Z. (2017) *In vitro* antioxidant activity, total phenolic and flavonoid contents of ethanol extract of stem and leaf of *Grewia carpinifolia*. *Beni Suef Univ J Basic Appl Sci*. 6(1):10-4. doi: 10.1016/j.bjbas.201 6.12.003.
38. Izadiyan, Z., Shameli, K., Miyake, M., Hara, H., Mohamad, S.E.B., Kalantari, K., Taib, S.H.M. and Rasouli, E. (2020) Cytotoxicity assay of plant-mediated synthesized iron oxide nanoparticles using Juglans regia green husk extract. *Arab. J. Chem.* 13: 2011–2023. Doi: 10.1016/J.ARABJC.2018.02.019
39. Wong, I., Li, H., Cheng, K. and Chen, F. (2006) A systematic survey of antioxidant activity of 30 Chinese medicinal plants using the ferric reducing antioxidant power assay. *Food Chem* 97: 705–711. https://doi.org/10.1016/j.foodchem.2005.05.049
40. Hongyan, X, L., Qiang, Z., Junyangli, J. D., Xiujian, C., Jun, T. C. X. (2014). Preparation Method of Co3O4 Nanoparticles Using Degreasing Cotton and Their Electrochemical Performance in Super Capacitor. *Journal of Nanoparticles* **4**(1):1-9. http://dx.doi.org/10.1155/2014/723057
41. Wadekar, K.F., Nemade, K. R., and Waghuley, S. A. (2017). Chemical Synthesis of Cobalt Oxide Nanoparticles Using Co-Precipitation Method. Research Journal of Chemical Sciences. 7(1): 53-55

International Journal of Current Science Research and Review
ISSN: 2581-8341
Volume 09 Issue 04 April 2026
DOI: 10.47191/ijcsrr/V9-i4-47, Impact Factor: 8.048
IJCSRR @ 2026
www.ijcsrr.org

42. Danbature, W. L., Isyaka M. Sani, Abdullahi M Abdullahi, Gambo, A. A. and Abdulmalik, S. S. (2023) UV-VIS, FTIR and XRD characterization of synthesized magnetic cobalt (Co_3O_4) nanoparticle used in catalytic decomposition of hydrogen peroxide. *FUDMA Journal of Sciences* (FJS) Vol. 7 No. 6, December 2023, pp 222 -227 DOI: https://doi.org/10.33003/fjs-2023-0706-2105
43. Suman, T. Y., Elumalai, D., Kaleena, P. K., and S. R. R. Rajasreea (2013) GC–MS analysis of bioactive components and synthesis of silver nanoparticle using Ammannia accifera aerial extract and its larvicidal activity against malaria and filariasis vectors, *Industrial Crops and Products*. 47: 239–245. https://doi.org/10.1016/j.indcrop.2013.03.010
44. Parethe, G. T., Rajesh, P., Nathiya, P., Balaji, M. and Kavica, S. (2023) Green synthesis of cobalt oxide nanoparticles from Clitoria ternatea flower extracts its characterization and biological activities. *World Journal of Advanced Research and Reviews.* 19(01): 001–009 doi.org/10.30574/wjarr.2023.19.1.1301
45. Du, H., Jiao, L., Wang, Q. Yang, J., Guo, L., Si, Y., Wang, Y. and Yuan, H. (2013) Facile carbonaceous microsphere templated synthesis of Co_3O_4 hollow spheres and their electrochemical performance in supercapacitors," Nano Research. 6(2): 87-98. https://doi.org/10.1007/s12274-012-0283-5
46. Wang, X., Yu, L, Wu, X. Yuan, F, Guo, Y, Ma, Y. and Yao, J. (2009) Synthesis of single-crystalline Co_3O_4 octahedral cages with tunable surface aperture and their lithium storage properties. *Journal of Physical Chemistry C.* 113(5):15553 – 15558. DOI:10.1021/JP904652M

Cite this Article: Otitolaiye, C., Ibrahim, B., Muhammad, M., Abdussalam, U. (2026). Free Radical Scavenging Potential of Cobalt Nanoparticles Synthesized from Ipomoea Batatas Leaves Extract. International Journal of Current Science Research and Review, 9(4), pp. 2148-2160. DOI: https://doi.org/10.47191/ijcsrr/V9-i4-47